Nonlinear resonant coupling between shear and heat fluctuations in fluids far from equilibrium

David Ronis
Department of Chemistry, Harvard University, Cambridge, Massachusetts 02138

Itamar Procaccia
Chemical Physics Department, Weizmann Institute of Science, Rehovot 76100, Israel

(Received 12 April 1982)

Fluctuating hydrodynamics is used to show that in fluids with large temperature gradients the shear mode couples to the heat mode in a resonant manner that results in a very large increase in the amplitude of the central peak of the spectrum of scattered light, in agreement with the results of Kirkpatrick *et al.* [Phys. Rev. A 26, 995 (1982)].

Recently, much attention has been devoted to the study of fluctuations in simple systems in nonequilibrium steady states (NESS).[1–10] With few exceptions,[5,8,9] most of the work has focused on systems close to equilibrium. Here we consider fluctuations around a steady state with large gradients, specifically large temperature gradients. As will be shown below, fluctuating hydrodynamics leads to a coupling of the shear to the heat mode which results in a large increase in the Rayleigh peak in the light scattering spectrum, in agreement with the results of Kirkpatrick, Cohen, and Dorfman.[8(b)–8(d)] Moreover, the enhancement is nonlinear in the gradients characterizing the steady state.

To see how the effect arises we start from the fluctuating nonlinear hydrodynamic equations linearized around the steady state with a fixed temperature gradient $\vec{\nabla} T$. We write the equations in terms of the pressure, temperature, and velocity fields, in Fourier representation. We denote $v^L_{\vec{k},\omega} = \vec{k}/k \cdot \vec{v}_{\vec{k},\omega}$ and $\vec{v}^t_{\vec{k},\omega} = (\vec{k}/k) \times \vec{v}_{\vec{k},\omega}$, where $\vec{k}$ is the wave vector and $\vec{v}_{\vec{k},\omega}$ is the Fourier component of the velocity field. The equations are

$$i\omega(\gamma_p \delta p_{\vec{k},\omega} - \gamma_T \delta T_{\vec{k},\omega}) = ik v^L_{\vec{k},\omega} + \gamma_T \vec{\nabla} T \cdot \vec{v}_{\vec{k},\omega} \ , \tag{1}$$

$$i\omega \vec{v}_{\vec{k},\omega} = \frac{i\vec{k}\delta p_{\vec{k},\omega}}{\rho_0} - k^2 \nu_t \vec{v}_{\vec{k},\omega} - \vec{k}\vec{k} \cdot \vec{v}_{\vec{k},\omega}(\nu_l - \nu_t) + \frac{i\vec{k} \cdot \vec{\tau}_{\vec{k},\omega}}{\rho_0} \ , \tag{2}$$

$$i\omega \left(\delta T_{\vec{k},\omega} - \frac{T\gamma_T}{C_p} \delta p_{\vec{k},\omega} \right) = - \vec{\nabla} T \cdot \vec{v}_{\vec{k},\omega} - \chi k^2 \delta T_{k,\omega} + i\vec{k} \cdot \vec{q}_{\vec{k},\omega} \ , \tag{3}$$

where the first equation comes from the continuity equation after the change of variable $\delta\rho = \rho_0(\gamma_p \delta p - \gamma_T \delta T)$, the second equation is the linearized Navier-Stokes equation $\nu_t = \eta/\rho_0$ and $(\nu_l - \nu_t) = (\zeta + \frac{1}{3}\eta)/\rho_0$, where η and ζ are the shear and bulk viscosities, ρ_0 is the mean density, and $\vec{\tau}$ is the random stress tensor. The third equation is the linearized heat conduction equation where χ is the thermal diffusivity, C_p is the heat capacity per unit volume, and $\vec{q}$ is the random heat flux. The use of such equations far from equilibrium has been discussed and justified in Ref. 1. By applying the projection operator $(1 - \vec{k}\vec{k}/k^2)$ to Eq. (2) we get a solution for $\vec{v}^t_{\vec{k},\omega}$:

$$\vec{v}^t_{\vec{k},\omega} = \frac{i\vec{k} \cdot \vec{\tau}_{\vec{k}} \cdot (1 - \hat{k}\hat{k})}{\rho_0(i\omega + \nu_t k^2)} \ , \tag{4}$$

where $\hat{k} = \vec{k}/k$. Using this solution for $\vec{v}^t_{\vec{k},\omega}$ we can write a 3×3 matrix equation for the variables

$$\underline{a} \equiv (\delta p_{\vec{k},\omega}, \delta T_{\vec{k},\omega}, v^L_{\vec{k},\omega})$$

in the form

$$\begin{pmatrix} i\omega\gamma_p & -i\omega\gamma_T & -(ik + \gamma_T \hat{k} \cdot \vec{\nabla} T) \\ \left(\frac{\gamma_p}{\gamma_T} - \frac{T\gamma_T}{C_p}\right) i\omega & \chi k^2 & -\frac{ik}{\gamma_T} \\ -\frac{ik}{\rho_0} & 0 & (i\omega + \nu_l k^2) \end{pmatrix} \cdot \underline{a} = \begin{pmatrix} \gamma_T \vec{\nabla} T \cdot (I - \hat{k}\hat{k}) \cdot \vec{\tau} \cdot i\vec{k} \\ \rho_0(i\omega + \nu_t k^2) \\ i\vec{k} \cdot \vec{q} \\ ik\hat{k}\hat{k} : \vec{\tau}/\rho_0 \end{pmatrix} . \tag{5}$$

We see that the source term on the right-hand side (RHS) of Eq. (5) has a pole at $\omega = k = 0$ which will be shown to significantly affect the central spectral line of scattered light. Note that this contribution comes from the coupling of the "transverse" velocity to the longitudinal modes. From Eq. (5) we can solve for $v^L_{\vec{k},\omega}$ quite easily. Then we can use the linearized continuity equation to write

$$\frac{i\omega\delta\rho_{\vec{k},\omega}}{\rho_0} = ikv^L_{\vec{k},\omega} + \gamma_T \vec{\nabla} T \cdot \vec{v}_{k,\omega} \ .$$

Once we decompose $\vec{v}_{k,\omega}$ into its transverse and longitudinal parts, and use Eq. (4), we get

$$\frac{i\omega\delta\rho_{\vec{k},\omega}}{\rho_0} = (ik + \gamma_T \hat{k}\cdot\vec{\nabla}T)v^L_{\vec{k},\omega} + \frac{\gamma_T \vec{\nabla} T\cdot(1-\hat{k}\hat{k})\cdot\vec{\tau}_{\vec{k},\omega}\cdot i\vec{k}}{\rho_0(i\omega + k^2\nu_t)} \ . \quad (6)$$

We can now employ the expression for $v^L_{\vec{k},\omega}$, which is obtained from Eq. (5), to write

$$\frac{\delta\rho_{\vec{k},\omega}}{\rho_0} = A_{\vec{k},\omega}\vec{\nabla}T\cdot(1-\hat{k}\hat{k})\cdot\vec{\tau}_{\vec{k},\omega}\cdot i\hat{k}/\rho_0 + B_{\vec{k},\omega} i\hat{k}\cdot\vec{q}_{\vec{k},\omega} + C_{\vec{k},\omega} i\hat{k}\hat{k}:\vec{\tau}_{\vec{k},\omega}/\rho_0 \ . \quad (7)$$

$$A_{\vec{k},\omega} = \frac{\{k^2/\rho_0 + (i\omega+\nu_t k^2)[\gamma_p\chi k^2 + i\omega(\gamma_p - T\gamma_T^2/C_p)]\}k\gamma_T}{(i\omega+\nu_t k^2)\Delta(k,\omega)} \ , \quad (8)$$

$$B_{\vec{k},\omega} = \frac{i(ik+\gamma_T\hat{k}\cdot\vec{\nabla}T)k^2\gamma_T}{\rho_0\Delta(k,\omega)} \ , \quad (9)$$

$$C_{\vec{k},\omega} = k(ik+\gamma_T\hat{k}\cdot\vec{\nabla}T)[k^2\gamma_p\chi + i\omega(\gamma_p - T\gamma_T^2/C_p)]/\Delta(k,\omega) \ , \quad (10)$$

where $\Delta(k,\omega)$ is the determinant of the matrix appearing in Eq. (5).

The calculation of the density autocorrelation function (and hence the light scattering intensity) follows when the random flux correlations are specified. From the work presented in Ref. 1, we know that a local equilibrium assumption should adequately describe these correlations. Physically, this is due to the fact that the random fluxes represent fast microscopic processes which have only to probe their local environment.

Thus[1,11]

$$\langle \tau^{ij}_{\vec{k},\omega}\tau^{lm*}_{\vec{k}',\omega}\rangle = (\delta_{il}\delta_{jm} + \delta_{jl}\delta_{im} - \tfrac{2}{3}\delta_{ij}\delta_{jm})\times\overline{(k_BT\eta)}_{\vec{k}-\vec{k}'} + \delta_{ij}\delta_{lm}\overline{(k_BT\zeta)}_{\vec{k}-\vec{k}'} \ , \quad (11)$$

$$\langle q^L_{\vec{k},\omega} q^{lm*}_{\vec{k},\omega}\rangle = 0 \ , \quad (12)$$

and

$$\langle q^L_{\vec{k},\omega} q^{j*}_{\vec{k}',\omega}\rangle = \delta_{ij}\overline{\overline{(k_BT^2C_p^{-1}\chi)}}_{\vec{k}-\vec{k}'} \ , \quad (13)$$

where $\overline{\overline{(\ )}}_{\vec{k}-\vec{k}'}$ is used to denote the spatial Fourier transformer at wave vector $\vec{k}-\vec{k}'$ of the quantity inside the brackets and where δ_{ij} denotes a Kronecker δ. In writing out Eqs. (11)–(13), overall factors of $(2\pi)^3$ have been dropped, since they are unimportant in measuring relative intensities.

In the experiment, the temperature profile is one dimensional (i.e., $\vec{\nabla}T \propto \hat{e}_3$; a unit vector in the z direction). From Eqs. (11)–(13), it follows that the components of $\vec{k}$ and $\vec{k}'$ orthogonal to $\vec{\nabla}T$ must be equal, since the system is translationally invariant in these directions. The calculation for $\vec{k}$ and $\vec{k}' \perp \vec{\nabla}T$ is simplified, although the essential novelties remain. Treating all material parameters as constants [with the exception of $T(z)$] and using Eqs. (7) and (11)–(13) gives

$$S_{\vec{k},\omega} \equiv \langle \delta\rho_{\vec{k},\omega}\delta\rho^*_{\vec{k},\omega}\rangle = |B_{\vec{k},\omega}|^2\frac{2\chi}{C_p}\overline{T^2} + \frac{2\bar{T}}{\rho_0}(\nu_l|C_{\vec{k},\omega}|^2 + \nu_t|\vec{\nabla}T|^2|A_{\vec{k},\omega}|^2), \quad \vec{k}\perp\vec{\nabla}T \ , \quad (14)$$

where the "bar" over T^2 and T denotes the spatial average of the quantity.

It is easy to see from Eqs. (8)–(10) and (14) that the Brillouin peaks have exactly the same structure as in equilibrium when $\vec{k}$, $\vec{k}' \perp \vec{\nabla}T$. The new features are contained in the central region of the spectrum, i.e., for $\omega \sim \chi k^2$, $\omega \ll kc_0$ where c_0 is the adiabatic sound speed. In this region,

$$A_{\vec{k},\omega} \sim ki\gamma_T(i\omega+\nu_t k^2)^{-1}(i\omega+\chi k^2)^{-1} \ , \quad (15)$$

$$B_{\vec{k},\omega} \sim ik\gamma_T(\omega - ik^2\chi)^{-1} \ , \quad (16)$$

$$C_{\vec{k},\omega} \sim \rho_0[k^2\gamma_p\chi + i\omega(\gamma_p - T\gamma_T^2/C_p)](\omega - ik^2\chi)^{-1} \ , \quad (17)$$

which, when used in Eq. (14), gives

$$S_{\vec{k},\omega} \propto \frac{2\chi\gamma_T^2\overline{T^2}k^2}{C_p(\omega^2+\chi^2k^4)}\left[1 + \frac{\bar{T}}{\overline{T^2}}\frac{C_p}{\rho_0}\frac{\nu_t}{\chi}\frac{|\vec{\nabla}T|^2}{(\omega^2+\nu_t^2k^4)}\right] \ . \quad (18)$$

The first term on the RHS of Eq. (18) is the usual equilibrium Rayleigh peak. The second term in nonlinear in the spatial gradients. How large is the term? For water at 20 °C, $\rho_0 = 10^3$ kg/m^3, $\nu_t \sim 10^{-6}$ m^2/sec, $C_p \sim 4.2\times10^6$ J/m^{3}deg, $\chi = 1.47\times10^{-7}$ m^2/sec (the Prandtl number $\nu_T/\chi \sim 7$). In Fig. 1, the exact spectrum is plotted [i.e., Eq. (14)] for a variety of temperature gradients. We have taken $\bar{T}/\overline{T^2} = (293$

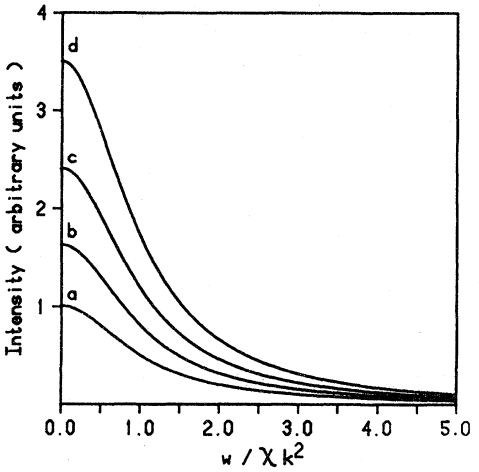

FIG. 1. Rayleigh peak (arbitrary units) for water at room temperature. The peak is symmetric about $\omega=0$. Temperature gradients were for curve a 0.0 K/cm, curve b 50 K/cm, curve c 75 K/cm, and curve d 100 K/cm. In all cases, $k=2500\ \mathrm{cm}^{-1}$.

$\mathrm{K})^{-1}$. This system corresponds to the one studied in Ref. 10. The effect is pronounced. As the temperature gradient increases, the overall intensity increases and the line narrows. From Eq. (18) we see that there is a strong ∇T dependence and an even stronger k dependence (i.e., k^{-4}).

In Eq. (5), we found that the effective longitudinal equations of motion do not have only random "white noise" sources. The coupling of the shear mode to the longitudinal variables by the temperature gradient produces a driving term whose power spectrum peaks exactly where the heat mode's does. This leads to a resonance which is reflected in the expression for the spectrum Eq. (18). Since it comes out so simply from the fluctuating hydrodynamical equations, its experimental verifications puts the applicability of these equations to fluids far from equilibrium to an important test.

The anomalies in the Brillouin peaks lead to no net increase in total intensity. This is not the case for the Rayleigh peak. From Eq. (18) it follows that the total intensity under the central peak is equal to

$$I_{\text{Rayleigh}} \propto \int_{-\infty}^{\infty} d\omega\, S_{\vec{k}\omega} = \frac{2\pi\gamma_T^2\overline{T}^2}{C_p}\left[1+\frac{\overline{T}}{\overline{T}^2}\frac{C_p|\vec{\nabla}T|^2}{\rho_0\chi(\chi+\nu_t)k^4}\right] . \quad (19)$$

Thus the contribution from the coupling to shear increases dramatically for small scattering angles (small k). In fact, in water (under the conditions described above) with $k=10^5\ \mathrm{m}^{-1}$ and $\nabla T=5000$ K/m, the new term is 24 times larger than the equilibrium term. Perhaps more important is the connection between the total central peak intensity and the static density autocorrelation function. In two dimensions (remember $k,k' \perp \vec{\nabla} T$) the inverse Fourier transform of Eq. (19) *grows* like r^2, while in three dimensions it grows like r.

We conclude this work with a few comments:

(1) Kirkpatrick, Cohen, and Dorfman,[8(b)–8(d)] using kinetic theory and mode coupling theory, have also examined the Rayleigh peak for large ∇T. The result derived here, i.e., Eq. (18), agrees with their calculation. It must be stressed that the fluctuating hydrodynamics calculation is quite different. Our basic equations [Eqs. (1)–(3)] are linear, the nonlinear equations having been linearized around the steady state. The justification for this is given in Ref. 1. Moreover, the fluctuating hydrodynamics approach has lead to a new simple explanation of the enhancement in the central peak, namely, the resonant coupling to shear fluctuations.

(2) In writing Eqs. (1)–(3), we have neglected the spatial variation of the coefficients. This is justified as long as they are constant over the mean free path of the modes (i.e., their decay length). For sound, a propagating mode, this poses some problems. On the other hand, for shear and heat modes (both diffusive), the typical decay length is $l \approx (\nu_t/\omega)^{1/2} \approx 10^{-3}$ cm in small-angle light scattering experiments. Thus the neglect of the spatial variation of the coefficients should be valid as long as $l|\nabla \ln T| \ll 1$ (for water at 300 K this implies $\nabla T \ll 3\times 10^5$ K/cm). This is easily satisfied in general.

(3) In establishing the connection between the light scattering intensity and the density autocorrelation function, some care must be exercised in treating the finite size of the incident beam. In short,[2,3,12,13] we require $l \ll$ the beam diameter, for $S_{k,\omega}$ to be simply proportional to the scattering intensity. This is a strong limitation for the Brillouin peaks ($l \sim 5$ cm) but not for the diffusive modes considered here ($l \sim 10^{-3}$ cm). In addition, the frequency resolution of today's experiments is not yet able to resolve the central peak. The width $2\nu_t k^2$ is about $10^4\ \mathrm{sec}^{-1}$ for the scattering angles under consideration. The total intensity is still measurable and thus the large enhancement should be observable.

(4) The effects of surfaces have been neglected. This is justified in the calculation of the spectrum since the modes under observation have extremely short decay lengths. [See point (1) above.] The total intensity involves an integration over all frequencies, the dominant contribution coming from $\omega \sim \nu_t k^2$ or χk^2. For large enough k, the decay length ($l \sim k^{-1}$) is small and the restrictions mentioned here and above are easily satisfied. On the other hand, as $k(l)$ is decreased (increased), either surfaces and/or the spatial variation of the coefficients discussed

above must be considered. The effect of surfaces has been considered in Ref. 12 for the Brillouin peaks. A strong dependence is found (l is large). The anomalies are much smaller when $l \gtrsim L$, the dimension of the sample. Since l for the central peak is roughly equal to k, we expect Eq. (19) to hold as long as $kL << 1$. Thus the growth of the static correlation will be modified by the surfaces when $k \sim L^{-1}$. We expect that as soon as $k \sim L^{-1}$ the static correlation will cease to increase. This was exactly the case for the Brillouin peaks.[12]

In summary, fluctuating hydrodynamics linearized about a NESS with a large temperature gradient has led to a simple explanation of the large enhancement in the Rayleigh peak. The temperature gradient causes shear mode fluctuations to drive in a resonant fashion, the heat mode, thereby causing the large intensity increase. This coupling not only changes the line shape, but changes the total integrated intensity and thus makes it experimental verification easier.

ACKNOWLEDGMENTS

This work has been supported in part by the U.S.-Israel Binational Science Foundation. One of us (D.R.) would like to thank the Chemical Physics Department of the Weizmann Institute for their hospitality while some of this work was being carried out.

[1]D. Ronis, I. Procaccia, and J. Machta, Phys. Rev. A 22, 714 (1980).

[2]A. -M.S. Tremblay, M. Arai, and E. D. Siggia, Phys. Lett. 76A, 57 (1980); Phys. Rev. A 23, 1451 (1981).

[3]D. Ronis and S. Putterman, Phys. Rev. A 22, 773 (1980).

[4]G. Van der Zwan and P. Mazur, Phys. Lett. 75A, 370 (1980); G. Van der Zwan, D. Bedeaux, and P. Mazur, Physica (Utrecht) 107A, 491 (1981).

[5]A. -M. S. Tremblay and C. Tremblay, Phys. Rev. A 25, 1692 (1982).

[6]I. Procaccia, D. Ronis, and I. Oppenheim, Phys. Rev. Lett. 42, 287 (1979); I. Procaccia, D. Ronis, M. A. Collins, J. Ross, and I. Oppenheim, Phys. Rev. A 19, 1290 (1979); D. Ronis, I. Procaccia, and I. Oppenheim, *ibid.* 19, 1307, 1324 (1979); 20, 2533 (1979).

[7]I. Oppenheim, in *Molecular Structure and Dynamics,* edited by M. Balabau (International Science Services, Jerusalem, Israel, 1980), p. 3.

[8](a) T. Kirkpatrick, E. G. D. Cohen, and J. R. Dorfman, Phys. Rev. Lett. 42, 862 (1979); 44, 472 (1980); (b) T. Kirkpatrick, Ph.D. thesis (Rockefeller University, 1981) (unpublished); (c) T. Kirkpatrick, E. D. G. Cohen, and J. R. Dorfman, Phys. Rev. A 26, 950, 972, 995 (1982); (d) E. D. G. Cohen, Kinam 3, 39 (1981).

[9]T. Kirkpatrick and E. G. D. Cohen, Phys. Lett. 78A, 350 (1980).

[10]D. Beysens, Y. Garrabos, and G. Zalczer, Phys. Rev. Lett. 45, 403 (1980); D. Beysens, in *NATO—Advanced Study Institute on Scattering Techniques Applied to Supramolecular and Nonequilibrium Systems, Wellesley, Massachusetts, August, 1980,* edited by S. H. Chen (Plenum, New York, 1981).

[11]L. D. Landau and E. M. Lifshitz, *Fluid Mechanics* (Pergamon, New York, 1959), Chap. 17.

[12]G. Satten and D. Ronis, Phys. Rev. A 26, 940 (1982).

[13]R. Edwards, J. Angus, M. French, and J. Dunning, J. Appl. Phys. 42, 837 (1971).